17th World Conference on Earthquake Engineering, 17WCEE
Sendai, Japan - September 13th to 18th 2020

INFORMING EMERGENCY RESPONSE OF HOSPITAL SYSTEMS AFTER MODERATE AND LARGE EARTHQUAKES IN LIMA, PERU

L. Ceferino[1,2], J. Mitrani-Reiser[3], A. Kiremdijian[4], G. Deierlein[4], C. Bambarén[5]

[1] *Post-doctoral Fellow, Civil and Environmental Engineering Department, Princeton University, e-mail: ceferino@princeton.edu*
[2] *Ph.D., Civil and Environmental Engineering Department, Stanford University*
[3] *Associate Chief of the Materials and Structural Systems Division, National Institute of Standards and Technology*
[4] *Professor, Civil and Environmental Engineering Department, Stanford University*
[5] *Professor, School of Public Health and Administration, Universidad Peruana Cayetano Heredia*

Abstract

Hospital systems are an important core of earthquake emergency response because these systems must provide timely treatment to people affected by the disaster. Earthquakes, however, can affect the hospitals' ability to function due to widespread damage to the hospital buildings and their supporting infrastructure. Additionally, earthquakes increase the demand for healthcare services as damaged urban infrastructure can cause injuries of high severity to people. The potential decrease in capacity and surge in demand for healthcare services can create a significant treatment shortfall throughout a city and subsequently increase the number of deaths during an earthquake aftermath. Thus, cities must develop proper preparedness and emergency plans to be able to respond to earthquakes with effective protocols for hospital systems. To address this problem, we use an earthquake emergency response model to design effective protocols for patient transfers and allocation of emergency response teams (EMTs) with field operating rooms for three earthquake scenarios in Lima, Peru. The model quantifies multi-severity earthquake casualties and captures reductions in the treatment capacity of hospitals. Earthquake magnitudes of 7.0, 8.0, and 8.8 are chosen to represent a range from moderate to large earthquakes in the central subduction zone of Peru. This paper describes the differences and similarities in deploying effective emergency plans for moderate and large earthquakes, indicating the critical regions that will need additional resources and the key roads to transfer patients. This study demonstrates that with proper planning, hospital systems can treat more injured people in a timely manner and with more efficient use of limited resources.

Keywords: earthquake resilience, emergency response, hospital systems, earthquake casualties, operating rooms.

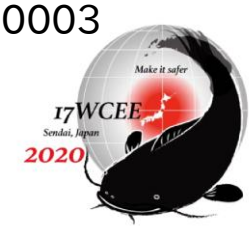

1. Introduction

Earthquake emergency response is a critical component of disaster risk management (DRM). During an earthquake emergency, thousands of people can suddenly require specialized medical treatment [1]. For example, the M 7.6 Kocaeli earthquake in Turkey injured around 50,000 people in 37 seconds [2]. Additionally, medium- and large-magnitude earthquakes can drastically reduce the hospitals' capacities. The Kocaeli earthquake heavily disrupted the functionality of ten major hospitals in Izmit requiring evacuations of most hospitals' inpatients [3]. Both the large increase in healthcare demand and the reduction in the capacity of hospital services put heavy strains on the hospital system, requiring emergency managers to prepare effective protocols to respond to the casualties with the limited resources.

Earthquake emergency response in large urban centers has an added complexity. Patients are mobilized from regions with healthcare delivery capacity to regions with high capacity through coordinated or uncoordinated patient transfers. For example, between 2,000 and 3,000 patients were transferred between hospitals after the M 8.8 2010 Chile earthquake [4]. Moreover, emergency managers deploy additional medical resources in the most affected areas as in the M 7.0 2010 Haiti earthquake, where foreign emergency medical teams deployed physicians and medical equipment in strategic regions [5]. Such a large patient mobilization and resource utilization in key regions demonstrate that hospitals in large urban centers behave as a system during an emergency response rather than as individual units working in isolation and responding locally.

Our recent study proposed a model to capture the critical factors of an earthquake emergency response in large urban centers: surge in casualties, reduction in hospital functionality, and system behavior [6]. The model includes a planning tool that finds optimal protocols to transfer patients between hospitals and to deploy field operating rooms in strategic locations. In the literature, there has been tremendous progress in characterizing emergency response and hospital functionality at the single hospital level using discrete-event simulation methods [7]–[10] and earthquake analytics to assess infrastructure vulnerability [11]–[14]. However, to the best of our knowledge, there are not available methods that capture emergency response at the system level.

In this paper, we apply our emergency response model to find optimal response protocols after three earthquake scenarios of magnitudes 7.0, 8.0, and 8.8 occurring in the subduction zone off the coast of Lima in Peru. Lima is a megacity with nearly 10 million people, where most healthcare services are managed by the Peruvian Health Ministry (MINSA) and Social Security (Essalud). Due to their treatment priority, we focused on patients severely injured who will require surgical procedures. Our previous study identified the optimal response for a single earthquake scenario of magnitude 8.0 [6]. In this paper, we extend the previous study to a wider range of earthquake magnitudes, covering both a medium-size rupture (M 7.0) and a scenario with the maximum observed magnitude in the region (M 8.8). We report the best transfer strategies between hospitals and the best locations to deploy field operating rooms for these three earthquake scenarios. Our goal is to create robust data that can inform emergency managers on strategies and plans to effectively respond to injured people in the aftermath of medium-size and large earthquakes.

2. Emergency Response Formulation

For paper completeness, we summarize our proposed emergency response model [6]. The model is based on a combination of an earthquake risk assessment and a proposed network flow model. The risk assessment is illustrated through the application in the next section and the network flow model is described here.

2.1.Network model

We model the patient treatment and transfers as a minimum cost time-varying network flow (MCTVNF) problem [15]. The full details of the model can be found in our previous study [6], thus we only provide a succinct description here. We use a directed graph to represent the hospital system and a discrete temporal representation of the emergency response with time steps dt equal to 1 day in a finite time horizon. Two nodes represent the triage and discharge nodes at each time step t, which belongs to the set T containing all discrete times within the time horizon. Triage nodes are defined with an integer index i, which takes values from 1 to n_h (represented by the set Γ), where n_h is the total number of hospitals in the system. The discharge nodes are

represented with index $j = i + n_h$, where i is the index of the hospital's triage node. The patients arriving at the triage nodes and leaving the discharge nodes are represented by the non-negative and negative flows $b_i(t)$, respectively, where i indicates the node index and t the time. The flow of patients within the system is represented by the variable $x_{i,j}(t)$. The flow $x_{i,j}(t)$ tracks patients transfers from triage node i to triage node j, and it also tracks patient treatment from triage node i to discharge node j. Travel times and treatment times are represented with the variable $\tau_{i,j}$. Additionally, patients waiting in triage node i at time t are represented by $y_i(t)$. Finally, the number of field hospitals deployed next to the hospital with triage node i is represented by the variable q_i.

Our previous study shows these variables can be used to build a network model that can capture patient mobilizations and represent the average patient waiting times and the average number of patients mobilized by ambulances in the left-hand and right-hand side of the objective function in Eq. (1), respectively [6].

$$C(X) = \alpha_1 \left(\frac{\sum_{t\in T} \sum_{\substack{i\in\Gamma; \\ j=i+n_h}} \{t + \tau_{i,j}\} \times x_{i,j}(t) \times dt}{\sum_{t\in T} \sum_{i\in\Gamma} b_i(t)} \right) + \alpha_2 \left(\frac{\sum_{t\in T} \sum_{i\in\Gamma} \sum_{j\in\Gamma} x_{i,j}(t) \times dt}{\sum_{t\in T} \sum_{i\in\Gamma} b_i(t)} \right) \quad (1)$$

The objective function contains two components weighted with α_1 equal to 0.9 and α_2 equal to 0.1, respectively, chosen through iterations in order to prioritize the reduction of waiting times over the efficient use of ambulances. The network constraints warrant that there is flow conservation, that the ambulance and operating room capacities are not exceeded even after deploying the additional field operating rooms, and that the flow of patients in the system is properly represented by positive numbers. The full constraint functions can be found in our previous study [6]. The equations in the objective and constraint functions are affine, therefore we can find the optimal protocol $\hat{X}$ in Eq. (2) using a linear programming solver [16].

$$\hat{X} = argmin_{x_{i,j}(t);y_i(t);q_i} C(X) \quad (2)$$

The optimal solution $\hat{X}$ will include the transfer and treatment strategies at each time step, the number of triaged people who will have to wait on-site before being treated, and the allocation of field operating rooms in the aftermath of the earthquake.

3. Application to the Subduction Zone off the coast of Lima, Peru

The emergency response model was applied to Lima under three earthquake scenarios occurring in the interface of the central portion of the Subduction Zone in Peru, where the oceanic Nazca plate and the continental South American plate converge. This portion of the Subduction Zone of Peru has generated massive historical earthquakes in the last 500 years [17]–[19]. These massive earthquake ruptures caused catastrophic consequences in Lima; however, the last large earthquake (M 8.0) occurred in 1974 [18], when Lima had only 3.5 M people, approximately a third of the current population of 10 M [20].

Since 1974, Lima has grown rapidly and exhibits large urban sprawl with residential infrastructure that often lacks engineering design according to the Peruvian Seismic Code [21]. The combined effect of the vulnerable infrastructure and the long seismic gap after the last large earthquake poses a high seismic risk in Lima.

The case studies in this paper examine the emergency response in Lima subjected to magnitudes of 7.0, 8.0, and 8.8 earthquakes. The catastrophe evaluation is based on a Monte Carlo simulation that uses 1,000 realizations to capture variability and interdependencies in the estimates of earthquake consequences for the three magnitudes.

3.1.Earthquake Scenarios and Shaking Intensities

The three earthquake scenarios assessed in this paper have a broad range of rupture sizes. Fig. 1a - c show the 2D projections of the rupture areas in red for magnitudes of 7.0, 8.0, and 8.8, respectively. The earthquake scenario of magnitude 8.8 replicated the historical earthquake in 1746 [22], whereas the earthquake scenario of magnitude 8.0 replicated the historical earthquake in 1940 [23]. The earthquake scenario of magnitude 7.0

was selected using the same epicenter coordinates as the scenario of magnitude 8.0 and with a focal depth of 45 km. The rupture areas are estimated from using empirical relationships between earthquake magnitude and rupture geometry [24], [25].

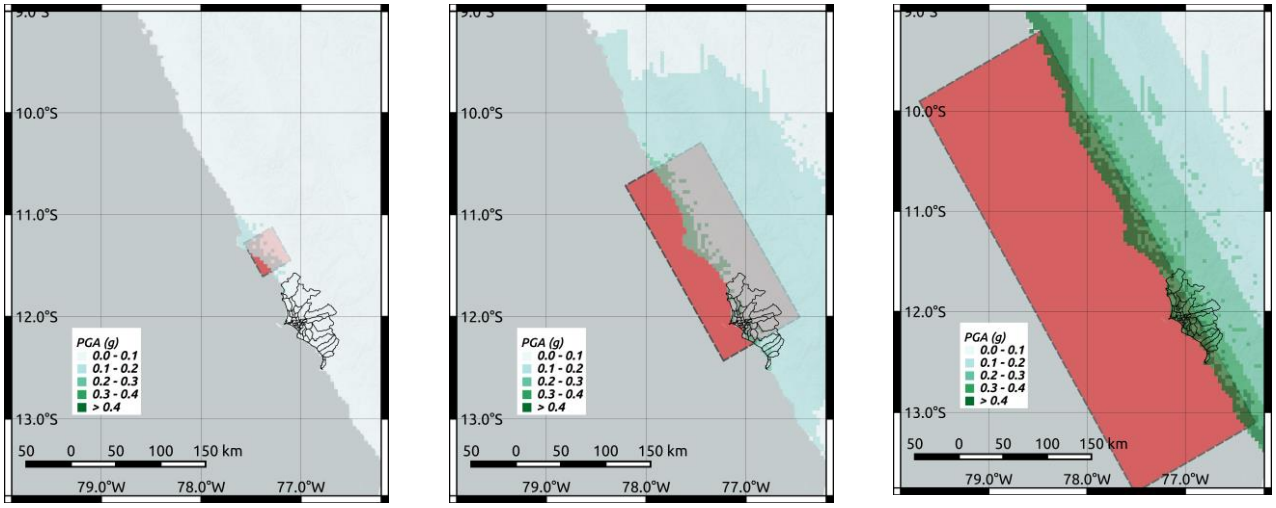

a) M 7.0 b) M 8.0 c) M 8.8

Fig. 1 – Earthquake ruptures and spatial distribution of median peak ground accelerations (PGA) for three earthquake scenarios in the Subduction Zone off the coast of Lima, Peru. Fig. 3a and 3c were adapted from our previous work [6], [26], [27]. Maps were created with QGIS software [28].

The ground shaking associated with each magnitude was estimated using ground motion prediction equations (GMPE) for interface ruptures in subduction zones [29], [30]. Three shaking intensities were evaluated to represent a wide range of structural typologies and periods of vibrations: peak ground acceleration (PGA), spectral acceleration at 0.3 seconds (Sa[0.3s]) and 1.0 seconds (Sa[1.0s]). Fig. 1a - c also show the spatial distribution of median PGA's, which captured shaking amplification due to the different soil conditions using data collected by [31]. Within-event and between-event standard deviations were also estimated with the GMPE's. A novel model to account for within-event spatial correlation with computational efficiency was also included to propagate empirically-observed spatial and across-period interdependencies [32]. Another existing model was also used to account for between-event correlations across structural periods [33].

3.2. The surge in Earthquake Casualties

The assessment of earthquake casualties was based on our previous study that extended the PBEE framework to account for spatially distributed multi-severity injuries and fatalities due to building damage [26], [27]. The analysis uses the information of 1.5M buildings gridded with a spatial resolution of 1 km by 1 km. This dataset was processed in our previous study [27] and was based on the structural typologies proposed by the Global Earthquake Model (GEM) as part of the South American Risk Assessment (SARA) [34]. Existing fragility functions for South America were used to capture the vulnerability of the structural typologies according to their material, structural system, and ductility levels [35]. The estimate of injured people who will need surgical procedures after the earthquake was estimated as 100% of people who will need to be treated immediately plus 10% of people who would need hospitalization but can wait to receive treatment. The epidemiology of these patients includes compound bone fractures or crush syndrome with exposed wounds. Our previous studies had already estimated multi-severity injuries for earthquakes magnitudes of 8.0 and 8.8 [6], [27], thus in this paper, we extended these results to include the scenario of magnitude 7.0.

The total number of earthquake casualties who will need surgical procedures are summarized in Table 1. The mean, median, and 10th and 90th percentiles are calculated from the 1,000 simulations of each earthquake magnitude. Our mean results indicate the 0.1k, 4.7k, and 19k people will require surgical procedures after the magnitudes of 7.0, 8.0, and 8.8, respectively. The wide range between the 10th and 90th percentile shows the large uncertainties in the estimates of earthquake patients as commonly found in catastrophe assessments.

Table 1 – Earthquake casualties needing surgical procedures after three earthquake scenarios in Lima

Earthquake Scenario	M 7.0	M 8.0	M 8.8
10th percentile	0	230	4,278
Median	17	2,170	15,689
Mean	121	4,725	19,347
90th percentile	250	12,438	40,421

The spatial distribution of patients is shown in Fig. 2. The sizes of the concentric circles indicate the mean number of patients at each of the 41 main hospital campuses in Lima. We assume that patients needing surgical procedures will arrive at the closest hospital. The plot shows how significantly larger the number of patients is for the larger magnitudes. Table 1 shows that the mean number of patients needing surgical procedures after the M 8.8 and M 8.0 earthquakes is 160 and 40 times larger than after the M 7.0 earthquake, respectively. Similar ratios between the number of patients for different magnitudes can be found in most hospitals.

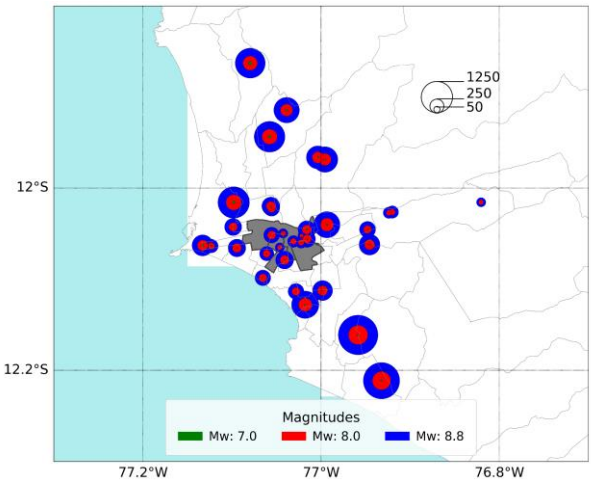

Fig. 2 – Location of patients needing surgical procedures for three earthquake scenarios in the Subduction Zone off the coast of Lima, Peru. Each circle represents the aggregated patients lumped at the locations of the closest hospital. Maps were created with Matplotlib and Basemap in Python [36].

3.3. Reduction in Hospital Functionality

The assessment of hospital functionality focused on the serviceability of operating rooms in the aftermath of earthquakes. We used the same methodology to determine functional operating rooms as our previous study [6], [37]. The methodology evaluates functionality uses a combination of structural vulnerability information and their Hospital Safety Index (HSI). HSI data enable us to incorporate multiple critical factors in the functionality assessment in addition to structural vulnerability, for example, the vulnerability of non-structural elements such as equipment or backup resources. The study leveraged key hospital infrastructure data surveyed by the Pontificia Universidad Católica del Perú (PUCP) and the World Bank [38]. The dataset included information of more than 700 buildings that belong to the most important 41 public hospital campuses in Lima.

Table 2 – Functional operating rooms after three earthquake scenarios in Lima

Earthquake Scenario	M 7.0	M 8.0	M 8.8
10th percentile	96	50	13
Mean	120	93	53
Median	122	97	51
90th percentile	142	128	96

The total numbers of functional operating rooms are summarized in Table 2. The mean, median, and 10th and 90th percentiles are estimated from the 1,000 simulations of each earthquake magnitude. Our mean results indicate that 120, 93 and 53 operating rooms will remain functional after the magnitudes of 7.0, 8.0, and 8.8, respectively. Conversely to the estimate of injuries, the 10th percentile of the distribution corresponds to a worst-case scenario rather than a best-case scenario. Larger shaking intensities reduce the number of functional operating rooms and simultaneously increase the number of patients. Because the model captures this effect, our results have a proper negative correlation between the patients needing surgical procedures and the functional operating rooms. Fig. 3 displays such a negative correlation in our results using a scatter representation of both quantities.

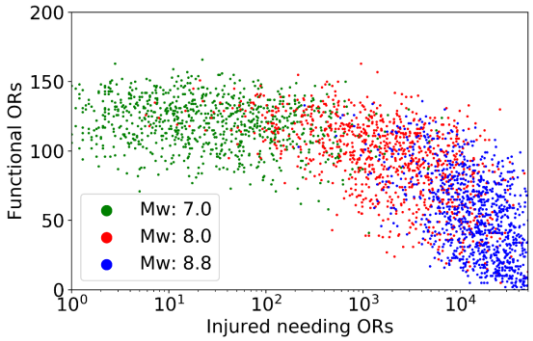

Fig. 3 – Scatter plot of patients needing surgical procedures and functional operating rooms in Lima. There are 1,000 dots in colors green, red and blue showing all the simulations for the three different magnitudes of analysis.

The spatial distribution of functional operating rooms is shown in Fig. 4. The concentric circles indicate the number of functional operating rooms in each of the 41 main hospital campuses in Lima. The white circles indicate the pre-event distribution of operating rooms, which amount to a total of 182. The green, red and blue circles show that the mean estimates of functional operating rooms are progressively reduced for larger magnitudes. Table 2 shows that the mean total numbers of functional operating rooms are 120, 93, and 53 (i.e., 66%, 51%, and 29%) of the total number of pre-event operating rooms for the scenarios of magnitude 7.0, 8.0, and 8.8, respectively. Similar ratios can be observed in individual hospitals in Fig. 4.

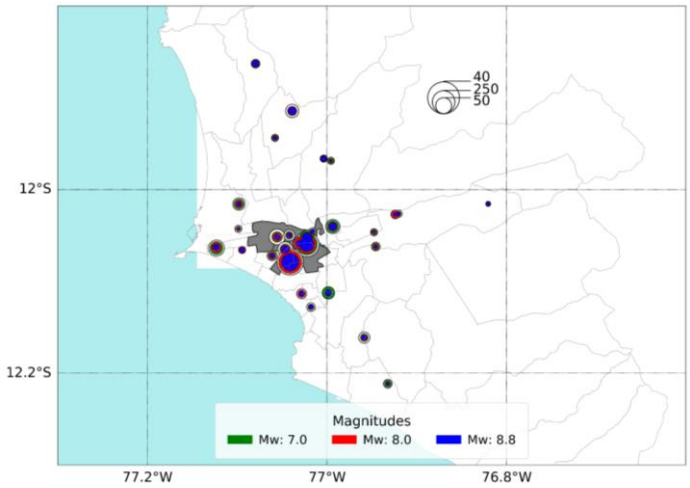

Fig. 4 – Spatial distribution of functional operating rooms in Lima after the three earthquake scenarios. Circles in colors green, red and blue show different earthquake magnitudes, and circles in white show operating rooms before being hit by the earthquakes. Maps were created with Matplotlib and Basemap in Python [36].

3.4. Spatial Mismatch in Demand and Capacity

The comparison between the spatial distribution of patients needing surgical procedures in Fig. 2 shows a clear contrast with the spatial distribution of functional operating rooms in Fig. 4. The urban layout of the city has

positioned most operating rooms at the center of the city, likely to facilitate accessibility to physicians living in higher-income neighborhoods better connected with the city center. In fact, under business-as-usual conditions, 95 operating rooms (52%) are located in the four centric districts shown in gray in Fig. 4: La Victoria, Breña, Jesús María, and Lima. Similar large concentrations of functional operating rooms are found in these four districts after the three earthquake scenarios. Table 3 reports mean estimates indicating that 53%, 59%, and 60% of the functional operating rooms will be located in these four districts after the earthquake magnitudes of 7.0, 8.0, and 8.8, respectively. Conversely, the concentration of patients needing surgical procedures is mostly at the periphery of the city, where vulnerable buildings are prevalent as a result of the lack of engineering design for seismic loads. In fact, Table 3 shows that only 10%, 13% and 12% of these patients will be located at the four centric districts, where the operating rooms are heavily concentrated, for the earthquakes of magnitudes 7.0, 8.0, and 8.8, respectively. Such a striking mismatch between the locations of high healthcare demand and capacity during the earthquake aftermath constitutes a tremendous challenge for emergency managers, who will have to create robust plans to connect the high-demand areas with the high-capacity regions of the city and/or to supply additional resources to the low-capacity zones.

Table 3 – Injured people needing operating rooms (ORs) and functional operating rooms within and outside four centric districts of Lima, Peru: La Victoria, Breña, Jesús María, and Lima. The numbers in parenthesis represent the absolute number of patients and operating rooms, respectively.

Earthquake Scenario		M 7.0	M 8.0	M 8.8
Within Lima Center	Casualties needing ORs	9.5% (12)	12.6% (595)	11.5% (2,229)
	Functional ORs	**53.2% (64)**	**58.9% (55)**	**60.1% (32)**
Outside Lima Center	**Casualties needing ORs**	**90.5% (114)**	**87.4% (4,125)**	**88.5% (17,118)**
	Functional ORs	46.8% (56)	41.1% (38)	39.9% (21)

3.5.Optimized Emergency Response with Effective Deployment of Field Hospitals

In this subsection, we quantify waiting times and describe the strategic use of key healthcare resources after deploying optimized, high-coordination emergency response protocols. We identify an optimal protocol using the emergency response planning tool discussed earlier. The tool uses linear programming to minimize patient waiting times and to effectively use ambulances [6]. Under the high-coordination plan, hospitals can share their ambulances across the entire city to mobilize patients from low-capacity regions to high-capacity regions. Additionally, the tool also finds the optimal locations to deploy 15 field operating rooms after each different earthquake scenario.

Our previous study showed that high-coordination response plans can reduce average waiting times by a factor of three with respect to low-coordination plans for the earthquake of magnitude 8.0 [6]. Instead of responding locally to the injuries under the low-coordination plan, hospitals respond globally under the high-coordination plan using effective transfer protocols. The optimal protocol solves the mismatch between demand and capacity by mobilizing patients from high-demand regions to high-capacity regions. Additionally, our previous study shows that under high-coordination plans, emergency medical teams (EMTs) will strategically deploy field operating rooms at the periphery where demands are the highest.

In this subsection, we extended this previous study to evaluate high-coordination emergency response for magnitudes of 7.0 and 8.8. We focused on high-coordination plans with the objective of reporting strategies that can serve as supporting information for emergency managers aiming to treat patients effectively and reduce waiting times, potentially saving lives. We ran the planning tool for each of the 1,000 simulations and estimated the average time that all patients have to wait across the city to be treated in each simulation. Using these simulations, Fig. 5 shows the distribution of average waiting time for each earthquake magnitude indicating the mean and 90th percentile. The scenario with magnitude 7.0 has very short waiting times for surgical procedures with a mean of three days. The distribution for this earthquake magnitude shows low probabilities for waiting times between 0 and 2 days because we assume that the patients take up to three days after the earthquake to arrive at the hospitals. Expectedly, the plot reports significantly longer waiting times

for larger magnitudes. The mean waiting time for the M 8.8 and M 8.0 earthquake is ~13 and ~3 times longer, respectively, than for magnitude M 7.0. Such striking increases arise from the significantly larger number of patients as reported in Table 1.

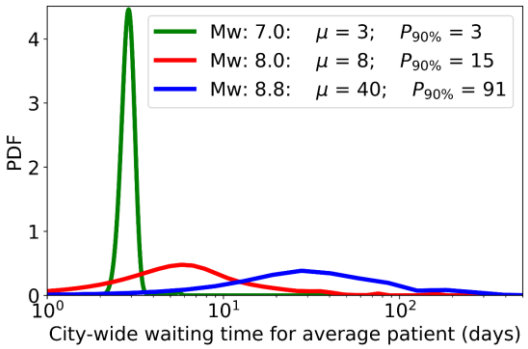

Fig. 5 – Distribution of city-wide average treatment times in Lima for three earthquake scenarios.

The optimized protocols for emergency response mobilize patients from low-capacity to high-capacity regions. Ideally, the number of treated patients in each hospital should be proportional to their available post-earthquake capacities. Fig. 6 shows the distribution of treated people at each hospital under the optimized protocol. Our previous study showed that under the optimized protocol, 48% of the patients where treated in the four centric districts after the earthquake of magnitude 8.0, where 50% of the functional operating rooms are located after deploying the 15 additional operating rooms in the periphery (see Table 3). Similarly, under the optimized protocol, 45% of the patients are treated within the four districts after the earthquake of magnitude 8.8, where 47% of the functional operating rooms are located. However, such an outcome does not hold for lower magnitudes. Under the optimized protocol, only 29% of the patients are treated in hospitals within the four centric districts even though more than 45% of the operating room resources are concentrated within them. On average, the M 7.0 earthquake scenario only has 121 patients who will need surgical procedures, significantly less than the M 8.0 and 8.8 earthquake scenarios. Thus, our planning tool effectively captures that the functional 120 operating rooms, on average, will be sufficient to treat patients locally in most districts, without the need of large mobilizations as in the M 8.0 and 8.8 earthquake scenarios.

The planning tool also finds strategic locations where EMTs should deploy field hospitals. Fig. 6a - c show these locations for the three earthquakes. The tool only locates field hospitals in close proximity to existing hospitals in order to increase their capacity and leverage key post-earthquake resources i.e., available hospital spaces or surplus medical equipment. The maroon and black colors indicate whether one or two field hospitals should be deployed. Because our assessment is probabilistic and uses linear programming, hospitals can have a mean number of field operating rooms represented by a fraction. The hospitals shown in orange have estimates close to 0 implying that the optimal protocol requires locating field hospitals in their close proximity. However, for simplicity, we only show mean estimates above 0.5, rounded to the closest integer.

Table 4 reports a ranking of the hospitals that need the largest number of field operating rooms under the optimized policy. The table indicates that very few field operating rooms need to be deployed for the scenario of magnitude 7.0. The emergency model assumes that field operating rooms need at least 3 days to be deployed, thus in multiple simulations, the post-earthquake capacity of operating rooms is enough to treat patients (see Fig. 7). In fact, on average, only 4 field operating rooms need to be deployed from a total of 15 available field hospitals. In contrast, the earthquake scenarios with magnitudes of 8.0 and 8.8 deploy the 15 field operating rooms in practically all the 1,000 simulations.

The top two hospitals in the list for the magnitudes of 8.0 and 8.8 are in the southern districts of Lima followed by other three hospitals in the northern districts. These results imply that the mismatch between demand and capacity can be slightly worse for the hospitals in the southern districts. However, it is important to consider that not all earthquake scenarios might result in similar outcomes. In fact, the three top hospitals for the earthquake of magnitude 7.0 are in northern districts because the ground shaking decays from North to South

for the magnitude 7.0 earthquake while the shaking is uniform from North to South for the magnitudes 8.0 and 8.8 (see Fig. 1).

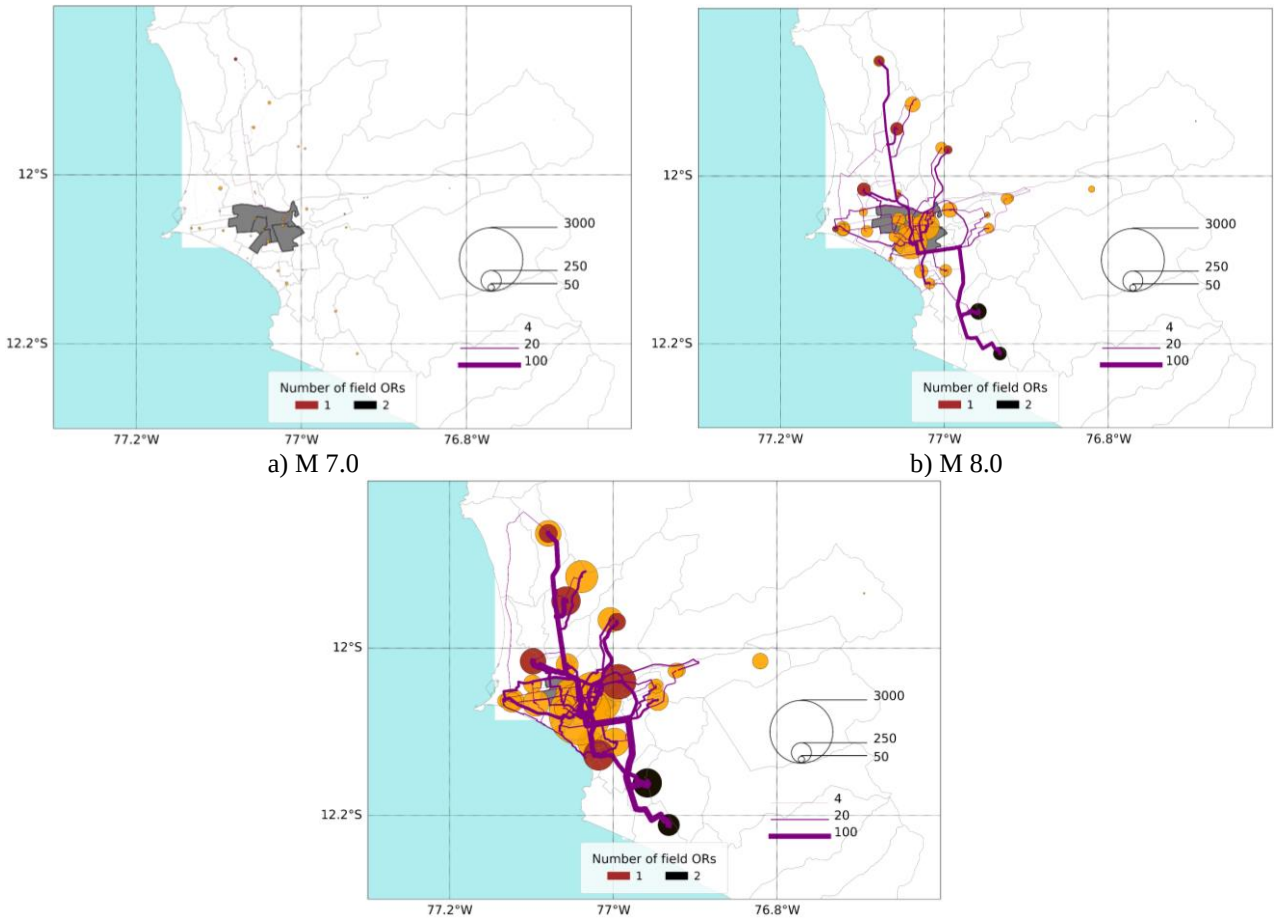

a) M 7.0 b) M 8.0

c) M 8.8

Fig. 6 – Spatial distribution of treated people at each hospital and total number of transfers in Lima after optimized emergency responses for different magnitudes. Maps were created with Matplotlib and Basemap in Python [36].

Table 4 – Ranking of five hospitals that need the largest deployment of field operating rooms for the three earthquake scenarios based on the mean number of deployed operating rooms rounded to the closest ingeter. Fractions smaller than 0.5 (shown in parenthesis) are rounded to 0. Hospital IDs: **A:** H. Uldarico Rocca (Villa El Salvador); **B:** H. María Auxiliadora (San Juan de Miraflores); **C:** H. Marino Molina (Comas); **D:** H. Carlos Lanfranco La Hoz (Puente Piedra); **E:** H. Luis Negreiros (Callao); **F:** Instituto Nacional de Rehabilitación (Bellavista)

M 7.0		M 8.0		M 8.8	
Hospital ID	N. field ORs	Hospital ID	N. field ORs	Hospital ID	N. field ORs
D	1	A	2	A	2
F	0 (*0.43)	B	2	B	2
C	0 (*0.30)	D	1	C	2
A	0 (*0.16)	C	1	D	1
B	0 (*0.14)	E	1	E	1

Finally, we report the top five pairs of hospitals with the largest number of patient transfers between them in Table 5. The scenario with magnitude 7.0 only requires few transfers because, as discussed earlier, the local response can be enough to treat the small number of patients requiring surgical procedures. However, the scenarios with magnitudes of 8.0 and 8.8 require the significantly larger mobilization of patients. The top three

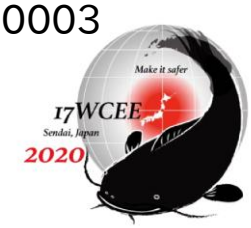

transfers in the scenario of magnitude 8.0 are from hospitals in the periphery of the city to one single hospital in the center of Lima, H. Edgardo Rebagliatti, which has the largest number of operating rooms. These top transfers are followed by a considerably large number of transfers from the periphery to the hospital with the second largest number of operating rooms, H. Guillermo Almenara, also located at the center of the city. For the magnitude 8.8 earthquake, the five top transfers are from the periphery to only one hospital, H. Edgardo Rebagliatti. These results indicate that H. Edgardo Rebagliati is of paramount importance for the earthquake emergency response of the city and that the treatment of multiple critically injured patients and their lives are dependent on this hospital's sustained functionality after earthquakes.

Table 5 – Ranking of patient transfers for the five pair of hospitals transferring the largest number of patients. The mean estimtates are reported and rounded to the closest integer. Hospital IDs: A: H. Uldarico Rocca (Villa El Salvador); B: H. María Auxiliadora (San Juan de Miraflores); C: H. Marino Molina (Comas); D: H. Carlos Lanfranco La Hoz (Puente Piedra); E: H. Luis Negreiros (Callao); F: Instituto Nacional de Rehabilitación (Bellavista); G: H. José Casimiro Ulloa (Miraflores); Y: H. Guillermo Almenara (La Victoria); Z: H. Edgardo Rebagliati (Jesús María).

M 7.0			M 8.0			M 8.8		
From (ID)	To (ID)	N. transfers	From (ID)	To (ID)	N. transfers	From (ID)	To (ID)	N. transfers
C	Z	1	B	Z	76	B	Z	135
D	Z	1	A	Z	72	A	Z	117
D	Y	1	D	Z	45	E	Z	110
D	E	1	A	Y	44	G	Z	101
C	Z	1	B	Y	43	C	Z	99

4. Conclusions

This paper presented the findings of applying an emergency response model for medium and large earthquakes in Lima, Peru. Earthquakes have caused emergency responses with thousands of people injured worldwide. Hospital systems must respond to these large numbers of injuries; however, they are also extremely prone to earthquake damage that can reduce their capacity rapidly. This paper provides a quantitative evaluation of earthquake emergency responses and strategizes protocols to effectively treat patients in large urban centers.

We summarized a recently proposed emergency response model and described how it captures three critical factors of earthquake emergency response in large urban centers: surge in earthquake casualties, the reduction of hospital functional, and system behavior. The high spatial resolution of the model enables us to identify the districts and neighborhoods particularly affected by high casualty rates and large reductions in the functionality of their hospitals. Additionally, the model introduces an optimization algorithm that evaluates best transfer strategies between hospitals and locates regions where field operating rooms to minimize patient waiting times.

This paper focused on injured people needing surgical procedures in the aftermath of earthquakes with magnitudes 7.0, 8.0, and 8.8 occurring in the Subduction Zone off the coast of Lima, a massive urban center with close to 10 M people. We assessed emergency responses for earthquakes occurring at nighttime to account for potential worst-case scenarios when people are at their residential buildings that often lack engineering design. Mean estimates indicate that there will be 0.1k, 4.7k, and 19.3k injured people needing surgical procedures after the earthquakes with magnitudes of 7.0, 8.0, and 8.8., respectively. Analogous estimates indicate that there will be only 120, 93, and 53 functional operating rooms for these three earthquake scenarios. The results capture the double adverse impact of large earthquakes on the hospital system and the emergency response: the number of injured people is significantly higher and the reduction in hospital functional is stronger for larger magnitudes.

We found a significant spatial mismatch between the location of injured people and the functional operating rooms after the earthquake. On average, 50% to 60% of the total functional operating rooms will be located in only four districts after the three earthquake scenarios. These four districts are concentrated in the center of the city. Conversely, the injured people needing operating rooms are mostly located at the periphery of the city.

In fact, on average, only 9% to 13% of these injured people are in these four districts, where the healthcare resources are heavily concentrated.

This paper evaluated optimized emergency responses to solve such spatial mismatch of post-earthquake healthcare demand and capacity. These optimized responses assume high coordination capacities between hospitals that enables them to share ambulance resources and strategize system-level protocols for patient transfers. Additionally, as part of these optimized responses, emergency medical teams will deploy 15 field operating rooms in key locations that are determined by the emergency response model.

Our mean estimates indicate that city-wide waiting times to treat patients will be 3 days, 8 days, and 40 days for the earthquake magnitudes of 7.0, 8.0, and 8.8, respectively. This paper reports the strategic locations to deploy field operating rooms for the three magnitudes. Also, it reports the pairs of hospitals that will need the largest number of transfers between each other. These results aim to support decision making during future earthquake emergency responses in Lima and other cities with similar urban layouts. While current earthquake emergency responses are considered to be haphazard, we deliberately evaluate optimized emergency responses and report their results to create key risk data that can support the construction of paradigmatic protocols aiming to reduce patient waiting times during earthquake emergency responses in large urban centers.

5. Acknowledgments

We acknowledge the financial support by the John A. Blume Fellowship from the Civil and Environmental Engineering Department at Stanford University and the Postdoctoral Fellowship at the Andlinger Center for Energy and the Environment at Princeton University.

6. Copyrights

7. References

[1] Centre for Research on the Epidemiology of Disasters, "EM-DAT | The international disasters database." Brussels, 2019.

[2] R. E. Reilinger *et al.*, "Coseismic and Postseismic Fault Slip for the 17 August 1999, Earthquake," *Science (80-.).*, vol. 289, no. 5484, pp. 1519–1524, 2000.

[3] R. C. Myrtle, S. F. Masri, R. L. Nigbor, and J. P. Caffrey, "Classification and prioritization of essential systems in hospitals under extreme events," *Earthq. Spectra*, vol. 21, no. 3, pp. 779–802, 2005, doi: 10.1193/1.1988338.

[4] American Red Cross Multi-Disciplinary Team, "Report on the 2010 Chilean Earthquake and Tsunami Response: U.S. Geological Survey Open-File Report 2011-1053 v1.1," Virginia, 2011.

[5] M. Gerdin, A. Wladis, and J. Von Schreeb, "Foreign field hospitals after the 2010 Haiti earthquake: How good were we?," *Emerg. Med. J.*, vol. 30, no. 1, pp. 1–5, 2013, doi: 10.1136/emermed-2011-200717.

[6] L. Ceferino, J. Mitrani-Reiser, A. S. . Kiremidjian, G. G. Deierlein, and C. Bambarén, "Effective Plans for Hospital System Response to Earthquake Emergencies," *Nat. Commun.*, vol. In review, 2019.

[7] J. A. Paul and L. Lin, "Impact of Facility Damages on Hospital Capacities for Decision Support in Disaster Response Planning for an Earthquake," *Prehosp. Disaster Med.*, vol. 24, no. 04, pp. 333–341, 2009, doi: 10.1017/S1049023X00007068.

[8] P. Yi, S. K. George, J. A. Paul, and L. Lin, "Hospital capacity planning for disaster emergency management," *Socioecon. Plann. Sci.*, vol. 44, no. 3, pp. 151–160, 2010, doi: 10.1016/j.seps.2009.11.002.

[9] M. Gul and A. F. Guneri, "A comprehensive review of emergency department simulation applications for normal and disaster conditions," *Comput. Ind. Eng.*, vol. 83, pp. 327–344, 2015, doi: 10.1016/j.cie.2015.02.018.

[10] A. H. Aghapour, M. Yazdani, F. Jolai, and M. Mojtahedi, "Capacity planning and reconfiguration for disaster-resilient health infrastructure," *J. Build. Eng.*, vol. 26, no. September, p. 100853, 2019, doi: 10.1016/j.jobe.2019.100853.

[11] G. P. Cimellaro, A. M. Reinhorn, and M. Bruneau, "Performance-based metamodel for healthcare facilities," *Earthq. Eng. Struct. Dyn.*, vol. 41, no. 11, pp. 1549–1568, 2011, doi: 10.1002/eqe.

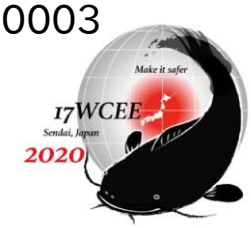

[12] S. Yavari, S. E. Chang, and K. J. Elwood, "Modeling post-earthquake functionality of regional health care facilities," *Earthq. Spectra*, vol. 26, no. 3, pp. 869–892, 2010.
[13] C. C. Jacques, J. McIntosh, S. Giovinazzi, T. D. Kirsch, T. Wilson, and J. Mitrani-Reiser, "Resilience of the canterbury hospital system to the 2011 Christchurch earthquake," *Earthq. Spectra*, vol. 30, no. 1, pp. 533–554, 2014.
[14] N. Tarque, H. Crowley, R. Pinho, and H. Varum, "Displacement-based fragility curves for seismic assessment of adobe buildings in Cusco, Peru," *Earthq. Spectra*, vol. 28, no. 2, pp. 759–794, 2012.
[15] M. Fonoberova, "Algorithms for Finding Optimal Flows in Dynamic Networks," in *Handbook of Power Systems II*, S. Rebennack, P. M. Pardalos, M. V. F. Pereira, and N. A. Iliadis, Eds. Springer, 2010.
[16] M. S. Andersen, J. Dahl, and L. Vandenberghe, "CVXOPT: A Python package for convex optimization, version 1.2." 2018.
[17] L. Dorbath, A. Cisternas, and C. Dorbath, "Assessment of the size of large and great historical earthquakes in Peru," *Bull. Seismol. Soc. Am.*, vol. 80, no. 3, pp. 551–576, 1990.
[18] L. Ceferino, A. Kiremidjian, and G. Deierlein, "Probabilistic space- and time-interaction modeling of mainshock earthquake rupture occurrence," *Bull. Seismol. Soc. Am.*, vol. In review, 2020.
[19] S. L. Beck and S. P. Nishenko, "Variations in the mode of great earthquake rupture along the Central Peru Subduction Zone," *Geophys. Res. Lett.*, vol. 17, no. 11, pp. 1969–1972, 1990, doi: 10.1029/GL017i011p01969.
[20] Macrotrends Inc., "Lima, Peru Population 1950-2020." [Online]. Available: https://www.macrotrends.net/cities/22078/lima/population.
[21] Ministerio de Vivienda, "Norma Técnica E.030 'Diseño Sismorresistente.'" Lima, Peru, 2016.
[22] S. Nishenko and R. Buland, "A generic recurrence interval distribution for earthquake forecasting," *Bull. Seismol. Soc. Am.*, vol. 77, no. 4, pp. 1382–1399, 1987.
[23] J. a. Kelleher, "Rupture zones of large South American earthquakes and some predictions," *J. Geophys. Res.*, vol. 77, no. 11, p. 2087, 1972,.
[24] D. L. Wells and K. J. Coppersmith, "New Empirical Relationships among Magnitude, Rupture Length, Rupture Width, Rupture Area, and Surface Displacement," *Bull. Seismol. Soc. Am.*, vol. 84, no. 4, pp. 974–1002, 1994.
[25] F. O. Strasser, M. C. Arango, and J. J. Bommer, "Scaling of the Source Dimensions of Interface and Intraslab Subduction-zone Earthquakes with Moment Magnitude," *Seismol. Res. Lett.*, vol. 81, no. 6, pp. 951–954, 2010.
[26] L. Ceferino, A. Kiremidjian, and G. Deierlein, "Probabilistic Model for Regional Multiseverity Casualty Estimation due to Building Damage Following an Earthquake," *ASCE-ASME J. Risk Uncertain. Eng. Syst. Part A Civ. Eng.*, vol. 4, no. 3, pp. 1–16, 2018.
[27] L. Ceferino, A. Kiremidjian, and G. Deierlein, "Regional Multi-severity Casualty Estimation Due to Building Damage Following a Mw 8.8 Earthquake Scenario in Lima, Peru," *Earthq. Spectra*, vol. 4, no. 3, 2018.
[28] QGIS Development Team, "QGIS Geographic Information System." Open Source Geospatial Foundation, 2009.
[29] J. X. Zhao *et al.*, "Attenuation relations of strong ground motion in Japan using site classification based on predominant period," *Bull. Seismol. Soc. Am.*, vol. 96, no. 3, pp. 898–913, 2006.
[30] N. Abrahamson, N. Gregor, and K. Addo, "BC hydro ground motion prediction equations for subduction earthquakes," *Earthq. Spectra*, vol. 32, no. 1, pp. 23–44, 2016.
[31] Z. Aguilar, F. Lazares, S. Alarcón, S. Quispe, R. Uriarte, and D. Calderón, "Actualización de la Microzonificación Sísmica de la cuidad de Lima," in *The International Symposium for CISMID 25th Anniversary*, 2013, no. 1, pp. 1–5.
[32] M. Markhvida, L. Ceferino, and J. W. Baker, "Modeling spatially correlated spectral accelerations at multiple periods using principal component analysis and geostatistics," *Earthq. Eng. Struct. Dyn.*, 2018.
[33] K. Goda and G. M. Atkinson, "Probabilistic characterization of spatially correlated response spectra for earthquakes in Japan," *Bull. Seismol. Soc. Am.*, vol. 99, no. 5, pp. 3003–3020, 2009.
[34] Global Earthquake Model, "South America Risk Assessment," 2013. [Online]. Available: https://www.globalquakemodel.org/what/regions/south-america/. [Accessed: 01-Feb-2017].
[35] M. Villar-Vega *et al.*, "Development of a Fragility Model for the Residential Building Stock in South America," *Earthq. Spectra*, vol. 33, no. 2, 2017.
[36] J. Hunter, "Matlplotlib: A 2D Graphics Environment," *Comput. Sci. Eng.*, vol. 9, no. 3, pp. 90–95, 2007.
[37] L. Ceferino, A. Kiremidjian, and G. Deierlein, "Computing Hospital System Resilience : a Supply-Demand Perspective," in *11th National Conference on Earthquake Engineering (NCEE)*, 2018.
[38] S. Santa Cruz, M. Blondet, A. Muñoz, J. Palomino Bendezú, and R. Tamayo, "Evaluación Probabilistica de riesgo Sísmico de Escuelas y Hospitales de la ciudad de Lima. Componente 2: Evaluación Probabilística del Riesgo Sísmico de Hospitales en la ciudad de Lima," Lima, Peru, 2013.

